MULTI-OBJECTIVE OPTIMIZATION OF BLAST SIMULATION USING SURROGATE MODEL

by

Toshihiro Tsuga

A Thesis
Submitted to the
Graduate Faculty
of
George Mason University
in Partial Fulfillment of
The Requirements for the Degree
of
Master of Science
Computational Sciences and Informatics

Committee:

_____	Director: Dr. Rainald Löhner
_____	Dr. Chi Yang
_____	Dr. Juan R. Cebral
_____	Dr. Fernando E.A. Camelli
_____	Dr. D. Papaconstantopoulos Department Chairperson
_____	Dr. Peter Becker Associate Dean for Graduate Studies, College of Science
_____	Dr. Vikas Chandhoke Dean, College of Science

Date: 12/7/07

Fall Semester 2007
George Mason University
Fairfax, VA

Multi-Objective Optimization of Blast Simulation Using Surrogate Model

A thesis submitted in partial fulfillment of the requirements for the degree of Master of Science at George Mason University

By

Toshihiro Tsuga
Bachelor of Engineering
Tohoku University, 2005

Director: Rainald Löhner, Professor
Department of Computational and Data Sciences

Fall Semester 2007
George Mason University
Fairfax, VA

ACKNOWLEDGEMENTS

I would like to thank my director, Professor Reginald Löhner, for his continuous and patient support in my research. His advice was always useful and made the execution of the research process smoother. As a researcher, I have learned many important things from him, which have affected my decision to pursue a future in scientific inquiry.

I would like to thank my parents who support my study abroad mentally and financially. It enabled me to concentrate on my study without any problems. My appreciation extends to all of my friends. They have always encouraged me whenever my research didn't go well and rejoiced my successes as if it was theirs. Being with them removed any anxieties and basketball games were always a good stress reliever.

TABLE OF CONTENTS

LIST OF FIGURES

ABSTRACT

MULTI-OBJECTIVE OPTIMIZATION OF BLAST SIMULATION USING SURROGATE MODEL

Toshihiro Tsuga, M.S.

George Mason University, 2007

Thesis Director: Dr. Rainald Löhner

A multi objective optimization approach using a Kriging model coupled with a Multi Objective Genetic Algorithm (MOGA) is applied to a blast damage maximization problem composed of two objectives, namely number of casualties and damage to buildings. The predicted Pareto front is located using a MOGA on the Kriging model. The location with maximum uncertainty along the Pareto front is added to the list of sample points. After each sampling, the Kriging model is reconstructed and this process is repeated until the maximum uncertainty is reduced.

The cases run show that the Pareto front is not always intuitively discernable. `Best locations' can vary significantly depending on the weight given to each optimization objective. The results also indicate that the effect of the additional cost incurred by the procedure to construct the `model of the model' totally compensates the computational expense.

1. Introduction

In this unstable situation of the world, the number of terror attacks in recent years has risen considerably. There are several popular ways of terrorizing - bomb, bio-arms, gas, airplanes, etc. The most common way of terror is by using explosives which not only kills people but also damages structures. Irrespective the final objective of individual acts of terrorism, in most cases the aim is to kill as many people as possible, destroy buildings of national importance, disable infrastructure and systems, and spread fear among people. To prevent such goals from materializing for terrorists, it is important to have knowledge about locations where maximum damage may be caused. This knowledge can help to protect buildings and, if this can not be avoided entirely, at least it helps minimize damage. Assuming that the purpose of a terrorist organization is to cause as much damage on people as on structures, the national defense organizations need to know about the blast locations where causes maximum damage. If only damage is of concern, such a place would be a location. On the other hand, if multiple destructive objectives are pursued (e.g. people killed and buildings destroyed), a trade-off between individual objectives has to be struck. This type of problem is known as multi objective problem. The example of typical multi objective problem is illustrated in figure 1-1. As one can see, it is not immediately clear which of the given solutions represent optimal solutions. One

way of defining optimality in a more precise way is via the concept of `dominated solutions'. A point is called "dominated" by another point when all objective values are smaller [1][37]. The set of non-dominated points is called the "Pareto front" or "Pareto solutions", and represents the set of optimal solutions. Hence, the main purpose of multi objective problem is to find such points. One can also see from Figure 1-1 that a single objective optimization would only search for solutions at the edges of the Pareto front, implying the need for multi-objective optimization techniques. In the following section, estimation methods of damages are presented.

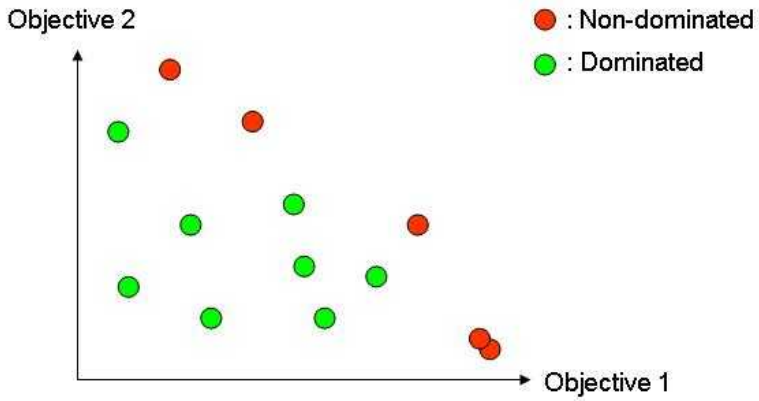

Figure 1-1 Example of typical multi-objective problem

1.1 Damage criteria

A traditional line-of-sight table look-up method gives a good estimate of such damages at a point visible from the blast location whereas at invisible places, where the shock waves refract, reflect and result in focusing on some places, it fails to evaluate correctly due to lack of physical models [31]. Especially, shielding effects which are known to reduce pressure and impulse is estimated poorly by these simple models [10]. Recently numerical simulation using 3D Euler flow solver have been replacing traditional methods. With the growth of computational power and the advances in Computational Fluid Dynamics (CFD), medium-fidelity 3-D blast runs with grids sizes of 10^6 elements can be computed in less than 8 hours in PC platforms.

The damage to people is mainly caused by shards of broken window glass cutting through people inside buildings. The estimation of casualties is difficult as it depends on the occupancy of buildings, which vary in time. In this study, the number of windows broken by pressure is used for the estimation. Window breakage is assumed to occur when either pressure or impulse exceed certain thresholds.

The structural damage to buildings depends on materials used, year of make, cracks caused by natural disaster (frequent earthquakes in Japan), which makes estimation difficult. Pressure on walls is assumed to be related to damage of structures. Like window breakage, the number of stations (probes) where pressure or impulse exceeds certain thresholds (much higher than window breakage case) is used as the damage criteria. This means that no coupling with Computational Structural Dynamics is conducted in this research.

1.2 Optimization method

Assuming that the amount of explosive is finite, and given the location of the explosion used as input, and the damages corresponding to the location become outputs. As mentioned above, the nature of shock wave (refraction, reflection, focusing) may produce worse damage at some location unexpectedly, making local extremes [39]. This means that traditional gradient-based methods will fail to find global optima. One alternative method is to use Genetic Algorithm (GA). Evolutionary Algorithms, particularly Genetic Algorithms (GA) [13] [18], firstly invented by J. Holland [19], are based on theory of evolution, where living things within populations evolve to fit an environment by crossover, mutation and selection. In the process of selection, the fitness which indicates how much the individual fits in the environment is usually considered. GAs have become one of the most popular Meta heuristic optimization methods. GAs are widely used due to their powerful skill to find global optima with little modifications needed for various problems, relative ease of coding, and convenience for parallelization. The application of GAs can be found in various engineering field ranging from the Traveling Salesman problem to optimization of wing shape [30] [35] [39]. Sasaki et al [34] conducted an optimization of SST wing shape using Multi-objective GA with Navier-Stokes code. As objective functions, drag for a transonic flow condition, drag for a supersonic cruise speed and bending moment at the wing root at the supersonic speed condition were used. As a result, the authors successfully obtained the shape with all three objectives improved to a basic shape. In this study, a total of 1,920 cases were computed using a

supercomputer. These papers show that GAs can find global optimization beautifully at a cost of many expensive evaluations.

1.3 Reducing the computational cost for optimization by using an approximation model

In order to alleviate the huge burden from GA, the method using response surface model (RSM) with GA has been developed recently [17][40].

Response surface method (RSM) [28] uses objective values of sampled points to predict objective value at an unknown point. RSM is a collection of statistical and mathematical techniques and it is useful for focusing on a region of interest as well as visualizing input-output relationship. The actual procedure is as follows. The response surfaces of the objective functions, two damages in this study, are reconstructed by fitting an approximation model (e.g. a polynomial function [20][32]) to data obtained by sampling in order to predict the objective value at unknown locations. The advantage of RSM is that it requires the fewest function evaluations among its alternatives [14]. Besides, the time to construct RSM is so little compared to expensive CFD computation that it can save a great amount of time even though a complex model is employed instead of a polynomial function. One of the downsides of this method is that in most of the cases we don't know which combination of what functions provides the most accurate prediction. Assuming one can find functions, the prediction by RSM still includes errors at unknown points.

This response surface method can be applied for GA as follows. The response surface model is constructed from initial sampled points. Then the GA searches for the global peak in the model, enabling to find the region of interest. Then some points in the region are sampled and the model is constructed again. This iteration is repeated until convergence of the model, or no further improvement is achieved. The problem of this method lies in the inaccuracy of the model. As one can see in figure 1-2, a model can easily miss a global peak, resulting in optimization of a local optimum. Therefore, this method is usually applied only to a small region of design space.

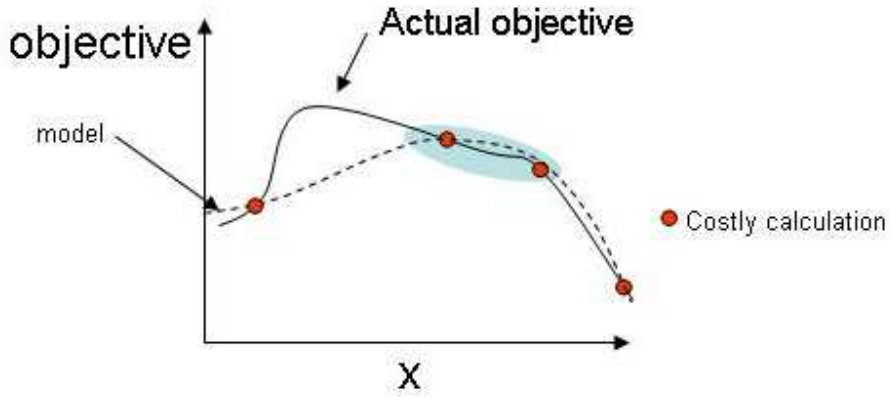

Figure 1-2 Example of how models miss a global optimum

The Kriging model was originally developed in the 1950s to estimate the location which had the maximum underground ore [12]. In the field of global optimization, where emphasis is put on searching sampling points, the history goes back to 1964 by H. Kushner. Kriging has been developed and applied many times since then [11][21][22][36][38][39].

The behavior of Kriging model is based on a stochastic process; estimating mean and distribution using sampled points assuming they have a Gaussian distribution. By harnessing this distribution, the Kriging model can predict uncertainty as well as objective functions at unknown points. One of the advantages is that one does not need to worry about choosing an inappropriate combination of functions. In the process of fitting the Kriging model to sampled data, the basis functions of the Kriging predictor change – Kriging is weighing mean method. The other advantage is that Kriging gives credible stopping criteria for additional sampling to improve the accuracy of the model. Expected improvement [14][21] measures how much a location is likely to become the global maxima by considering the objective function and uncertainty at the same time. By diminishing expected improvement to zero through iteration, we know stochastically no more improvement in maximum value can be expected. At this point, the Kriging model is so accurate that there is far less possibility to miss a global optimum of each objective. At this point, there might be a gap between the predicted Pareto front and the Pareto front of samples. Figure 1-3 illustrates this situation. The objective of a multi objective problem is to find out a global Pareto front. The point with the highest uncertainty among the Pareto solutions predicted by the Kriging model is sampled iteratively until a maximum uncertainty is reduced (more than 30% for the cases shown in this work). By doing this, uncertainties in the prediction decrease, and hence a more accurate prediction of the Pareto front can be obtained. If this approach is solely applied to the Kriging model without maximizing each objective using expected improvement, the possibility of obtaining local Pareto front instead of global Pareto front becomes much higher. In order

to capture the Pareto front correctly, Multi Objective GA (MOGA) is employed to this model instead of Single Objective GA. By adding this procedure, the entire region of the Pareto front will become accurate, providing designers a more reliable Pareto front.

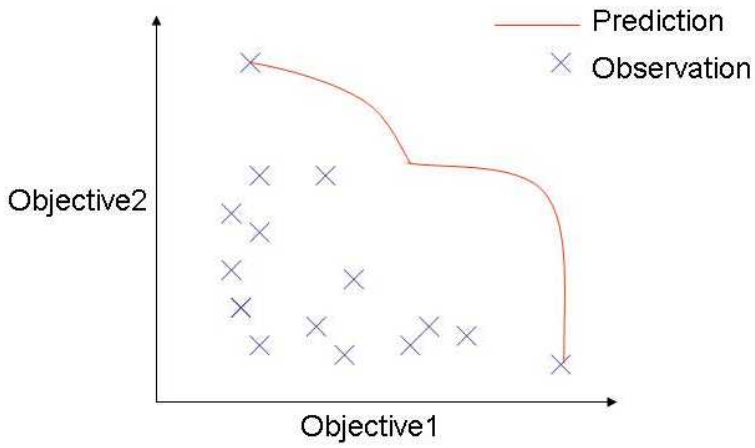

Figure 1-3 A predicted Pareto front and observations

1.4 Objective of this work

The main objective of this work is to establish a general method of optimization for multi objective functions applied to blast simulation. The entire procedure is illustrated in figure 1-4. The first process is identical to finding a global optimum of each objective. In multi-objective optimization, the point that designers usually care about is not the one with the extreme (best and poor combination) but the one that is more balanced - unless balanced points are really bad. The aim is to find such balanced points directly. However, since often those points are associated to extremes, it is necessary to go through the first stage beforehand. In the second process, MOGA is applied to those points by developing

a Kriging model. This procedure increases the accuracy of the middle part of the Pareto front. By going through those two stages, the entire region of the Pareto front becomes accurate.

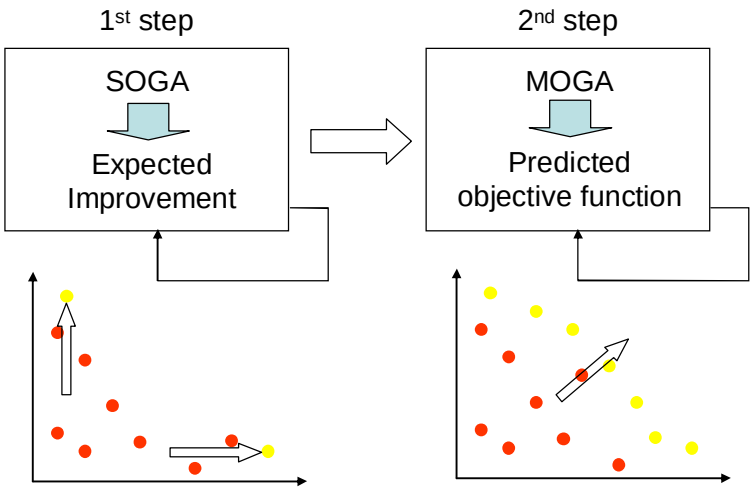

Figure 1-4 Entire procedure

Chapter 2 presents details about the GA (single and multi-objective). The mathematical equations and numerical implementations for the Kriging method as well as the flow solvers used in this study are presented. Chapter 3 presents the application of the Kriging method to analytical functions to carry out the entire process. The main purpose of this chapter is to debug and develop the Kriging code before the real experiment. In Chapter 4, the optimization with Kriging model is applied to blast simulation. Chapter 5 concludes this research.

2. Methodology

2.1 Genetic Algorithm

In this study, a Genetic Algorithm (GA) is employed to maximize the so-called Expected Improvement. GA is based on the theory of evolution. Like humans, all of the living things live not by themselves but rather live in populations. The diversity and strength of a population gives a better chance to survive as a species. A population with uniform individuals would become extinct easily by some singular event. There is always competition inside a population. In nature, an individual that is highly adapted to its environment is more likely to survive, mate, and reproduce. On the other hand, individuals who poorly adapt to their environment do not survive. The offspring from the individual with high adaptation are likely to inherit the property. As generations evolve, the entire population becomes more suited for the environment.

A genetic algorithm initially creates a set of individuals (population). Each individual is embedded with a unique chromosome that corresponds to the design variables. In order to represent how much an individual fits to the environment, the ‘fitness’ is calculated by using the objective values of the individual. Then parents are selected using fitness and those parents are crossed over - sometimes mutation occurs at these points (crossover, mutation). Finally, individuals who survive the next generation are selected according to their fitness. This flow chart is illustrated in figure 2.1

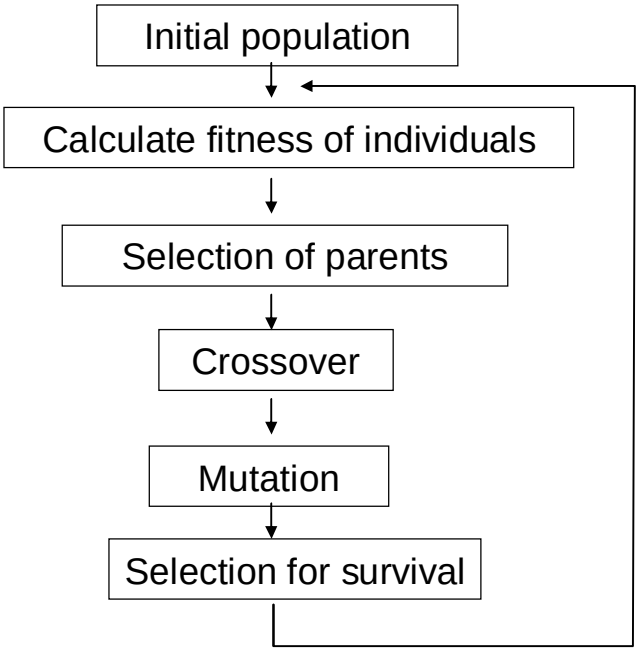

Figure 2-1 Procedure of Genetic Algorithm

2.1.1 Chromosome

There are two ways of represent design variables. In phenotypic representation, individuals represent solutions internally exactly as they are represented externally. Genotypic representation discretizes a value into binary coding (figure 2-2). Coding design variables in binary representation is somewhat different from phenotypic representation.

In phenotypic representation, unless one applies parameter constraints, the search area automatically moves. Unlike this, in genotypic representation, once one decides a range of design space to be discretized, the genetic algorithm is never able to create individuals outside this area. The behavior of binary GA is different from the other.

With a phenotypic approach, crossover is interpolation (extrapolation depending on a scaling parameter) of parents (figure 2-3). Whereas a genotypic approach, crossover can result in the creation of new parameter value by combining some of the bits from one parent with bits from the other (figure 2-4). Similarly with a phenotypic representation, a mutation results in a perturbation of a parameter value which with high probability is a small perturbation. With a genotypic representation, mutation involves flipping one of the bits of an encoded parameter value. This can make either a small or large perturbation depending on the order of the bit. This makes the behavior more explorative with a simple implementation.

In this research, binary representation is employed in order to explore the multi-peaked Expected Improvement surface.

	min		max
Actual value	0.	~	100.
Binary	00000	~	11111

Figure 2-2 Example of genotypic representation

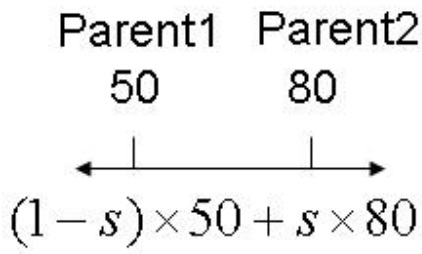

Figure 2-3 Example of typical phenotypic crossover

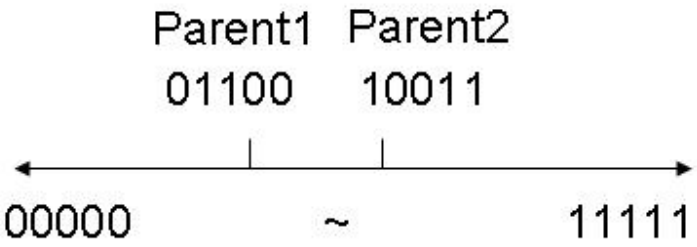

Figure 2-4 Example of uniform binary crossover

2.1.2 Selection

There are several popular ways to select individuals among population but most of them are based on fitness value. With deterministic methods, each individual is assigned a number corresponding to how many times they are to be selected. One of them is called truncation method where individuals with top m fitness survive. With stochastic methods, each individual is assigned probability based on which the individual is selected. Fitness proportional is one of the methods where probability is assigned proportional to its fitness. Another example is uniform probability where uniform probability is assigned. The effect of selection on behavior of GA is discussed in K.Dejong [23].

In this research, fitness proportional and truncation were used for parents and survivor selection respectively.

2.1.3 Crossover and Mutation

Crossover is a recombination process of parents. For example, parent1 [0,0,0] and parent2 [1,1,1] in binary representation possibly produce a offspring in any value between them with uniform crossover method. The basic idea is that crossover operation creates offspring between two parents.

In binary representation, crossover operator recombines sub-segments of parents. As the number of points to be subdivided increases, similarity between parents and offspring decreases if individuals in a population are heterogeneous. However, this variation becomes less effective as a population comes down to convergence. On the other hand, mutation introduces variations in offspring chromosomes every generation. Binary mutation employs Bitflip method. This method chooses binary bits stochastically and flips them. For example,

Before: 0101110 After: 0111010

Obviously, the more number of bits are mutated, the greater the variation the offspring gets.

Crossover can help produce variation in chromosome at a primitive generation. This is because individuals in those populations are diverse from each other (heterogeneous). After many generations, the individuals become similar each other (homogeneous). This

may cause convergence in sub-optimal peak in highly multi-modal surface. By adding a mutation process, the GA keeps exploring the design space.

In this research, all digits are sub-segmented (uniform crossover) for recombination to increase exploration and normal Bitflip method is employed for mutation.

2.2 Multi Objective Genetic Algorithm (MOGA)

A standard technique to handle a multi-objective technique is to convert it to a single objective problem by using a weighted sum of all objectives [37].

$$F(x) = \sum_{i=1}^{k} w_i F_i(x)$$

The advantage of using this method is that one can use a single objective approach exactly in the same way as for single objective optimization. The drawback is that there is no exact way to know the appropriate weights for each objective. One engine designer might think fuel efficiency is twice as important compared to torque, but he might think differently after several years. Therefore, a new technique to handle multiple objective functions equally is required.

There is a notion of a non-dominated solution [1] [37]. According to this paper, an individual x1 is said to dominate the other solution x2, if both the following conditions are true

1. The solution x1 is no worse than x2 in all objectives, $f_k(x_1) \geq f_k(x_2)$, for all k=1, …, M.

2. The solution x1 is strictly better than x2 in at least one objective, or $f_k^*(x_1) > f_k^*(x_2)$ for at least one $k^* \in \{1,...,M\}$.

A non-dominated individual is one that is not dominated by any others. A set of such non-dominated individuals are called “Pareto solutions” and the surface made of them are called “Pareto front”. The black dots in figure 2-5 are Pareto solutions, which are not dominated by any other individuals. A designer selects from the Pareto front the best match for the case of land. Figure 2-6, a close-up of dashed square area, illustrates that this green individual is dominated by three other individuals.

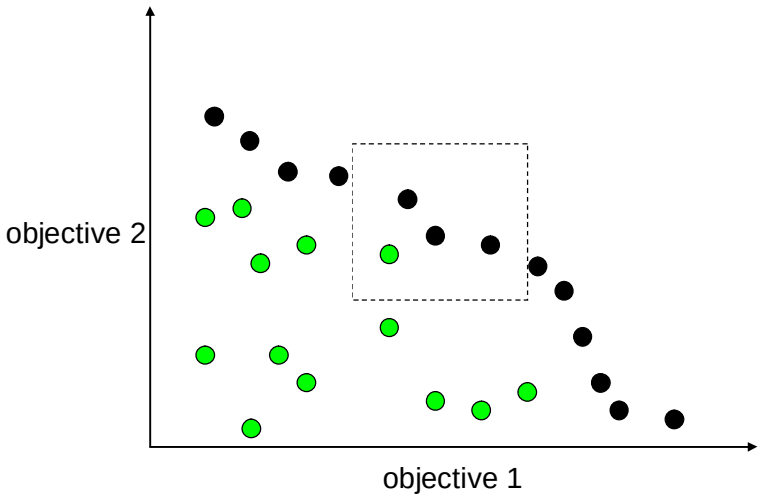

Figure 2-5 Illustration of non-dominated solutions

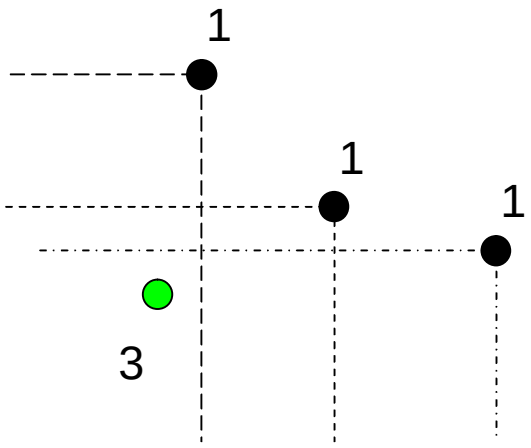

Figure 2-6 Illustration of non-dominated solutions

The solutions of MOGA are not an individual but a family of individuals known as the Pareto-optimal set or Pareto solutions. The following features are desired for the evaluation method of MOGA [29].

1. the solutions obtained are among Pareto-optimal
2. the solutions are uniformly sampled from Pareto-optimal set

The so-called Pareto ranking method [15] satisfies these features. A rank is given by

$$rank(x_i, t) = 1 + p_i^t$$

Here t is the number of generation, x_i is ith individual and p_i^t is number of individuals that dominate x_i. In this study the Pareto ranking method is employed to calculate fitness.

2.3 Response Surface Model

In this section, approximation methods (polynomial and Kriging) are presented followed by an explanation of the optimization approach by Kriging. Polynomial approximation is presented in order to compare it with Kriging model.

2.3.1 Polynomial Approximation

RSM with polynomial approximation have been applied for many examples including computer experiments [20][32][26] . The approximation model assumes the observation as a stochastic process; the equation consists of a regression and an error term as following.

$$y(x^i) = \sum_h \beta_h f_h(x^i) + \varepsilon^i \quad (i = 1,..., n). \tag{2-1}$$

Here each f_h is a basis function of x, β_h is the coefficient to be estimated and ε is a normally distributed independent (random) error term. The main objective of this approach is to fit functions into the observations by adjusting each coefficient of a function. The residual ε, on the other hand, is just treated as noise which is tried to be minimized for a best fitting of this model.

Let us suppose that we are dealing with computer experiments which have deterministic output. In other words, there are no measurement errors. The problem of using this approximation technique in computer experiment is that the residual term ε is independent with change in design space.

2.3.2 Kriging Interpolation

In contrast, interpolation methods treat an observation as a deterministic process. Kriging interpolation, which is based on statistical approach, was originally invented to find valuable underground mineral resources in 1951 by D. G. Krige [27], a South African geologist. Later, G. Matheron formalized his work and called the method Kriging to honor him [16]. Kriging model estimates a function (response surface) assuming it follows Gaussian distribution.

$$y(x^i) = \mu + \varepsilon(x^i) \quad (i = 1,...,n). \tag{2-2}$$

In this equation, μ is a linear regression, $\varepsilon(x)$ is the left-out term after the regression and n is a number of sample points. In computer experiments, there is no random error (measurement noise) hence ε solely indicates modeling error of the regression. Besides, if y(x) is continuous, $\varepsilon(x)$ is also continuous because of $\varepsilon(x) = y(x) - \mu$. Therefore, it is unrealistic to assume that $\varepsilon(x^i)$ and $\varepsilon(x^j)$ are independent of each other, rather that they are least in a continuity relationship. Intuitively, the closer x^i and x^j are the higher the correlation of $\varepsilon(x)$ should be. The main effort in Kriging approximation is to interpolate the error term $\varepsilon(x)$ based on stochastic behavior. The Kriging approach uses the following to measure a distance rather than the Euclidian distance because the latter weighs all variables equally.

$$d(x^i, x^j) = \sum_{h=1}^{k} \theta_h \mid x_h^i - x_h^j \mid^2 \quad (\theta_h \geq 0). \tag{2-3}$$

Here k is dimension of design space, θ_h is a parameter to be optimized. Using this distance, correlation of error term is calculated as follows.

$$Corr[\varepsilon(x^i),\varepsilon(x^j)] = \exp[-d(x^i,x^j)] \tag{2-4}$$

If two points are close, the correlation is about 1 (strong correlation). If two points are far apart, the correlation of $\varepsilon(x)$ is about 0 (weak correlation).

There are k parameters to be determined for a best fitting. The likelihood function is used to estimate its fitting.

$$\begin{aligned} Ln(\hat{\mu},\hat{\sigma}^2,\theta) = &-\frac{n}{2}\ln(2\pi) - \frac{n}{2}\ln(\hat{\sigma}^2) - \frac{1}{2}\ln(|R|) \\ &-\frac{1}{2\hat{\sigma}^2}(y-\vec{1}\hat{\mu})'R^{-1}(y-\vec{1}\hat{\mu}) \end{aligned} \tag{2-5}$$

Here n is a number of sampled points, R is a $n \times n$ matrix whose (i,j) element is $Corr[\varepsilon(x^i),\varepsilon(x^j)]$, $y = [y(x^1),....,y(x^n)]'$, $\vec{1}$ is n dimensional unit vector. The parameters μ and σ^2 that maximize likelihood function are defined as follows.

$$\hat{\mu} = \frac{\vec{1}'R^{-1}y}{\vec{1}'R^{-1}\vec{1}} \tag{2-6}$$

$$\hat{\sigma}^2 = \frac{(y-\vec{1}\hat{\mu})'R^{-1}(y-\vec{1}\hat{\mu})}{n} \tag{2-7}$$

By substituting (2-6) and (2-7) into (2-5), the likelihood function becomes function of only θ. Finally, Kriging predictor with these properties is represented as follows [33].

$$\hat{y}(x^*) = \hat{\mu} + r'R^{-1}(y-\vec{1}\hat{\mu}) \tag{2-8}$$

Here $r = Corr[\varepsilon(x^*),\varepsilon(x^i)]$ $(i = 1,....,n)$. The θ which maximize likelihood function is the parameter of the best fitted correlation to sampled data which is assumed as Gaussian. This Gaussian property is inherited in (2-8) through θ. Thus, Kriging model behaves as Gaussian.

2.3.2.1 Expected Improvement

Let us take a look at example (figure 2-7). The red dots represent sampled points, the dotted line is the Kriging prediction for the observation, the solid line is the actual objective function and the line at the bottom is uncertainties estimated using a Kriging predictor. In a maximization problem, optimization only depending on Kriging prediction will miss a global maximum. With uncertainty (error) information, we would have higher possibility of finding global optima. Kriging model can estimate uncertainty by utilizing statistical properties. Uncertainty of Kriging model is expressed as follows.

$$s^2(x^*) = \hat{\sigma}^2 \left[1 - r' R^{-1} r + \frac{(1 - \vec{1}' R^{-1} r)^2}{\vec{1}' R^{-1} \vec{1}} \right] \tag{2-9}$$

s^2 is a mean squared error of the predictor, which indicates an uncertainty at unknown points. This expression has the property that we want it to have: the closer a prediction point is to a sample point, the more accurate the prediction is. As the prediction moves away from the sample points, then the uncertainty at the point approaches to $\hat{\sigma}^2$. Each objective function has a corresponding uncertainty. With weaker correlations with nearby points than the other objective, the uncertainty of the objective function becomes higher. The combination of Kriging prediction and its uncertainty is known as expected improvement. The concept of expected improvement is illustrated in figure 2-8 where $f_{\max}$ is the maximum value among sampled points, distributions drawn vertically at x^i and x^j represents $Gaussian(\hat{y}(x^i), s^2(x^i))$ and $Gaussian(\hat{y}(x^j), s^2(x^j))$ respectively. At x^i, because both the predicted value and uncertainty are moderate, there is no possibility

to improve $f_{\max}$. At x^j, on the other hand, there is a possibility to make an improvement, where both the predicted value and uncertainty are relatively high. If a distribution at a given point exceeds $f_{\max}$ just as at x^j, improvement is expected. This property is expressed as the following equation.

$$E[I(x^*)] = (\hat{y} - f_{\max})\Phi\left(\frac{\hat{y} - f_{\max}}{s}\right) + s\phi\left(\frac{\hat{y} - f_{\max}}{s}\right) \tag{2-10}$$

Here $\Phi(\cdot)$ and $\phi(\cdot)$ are the distribution and standard normal density function.

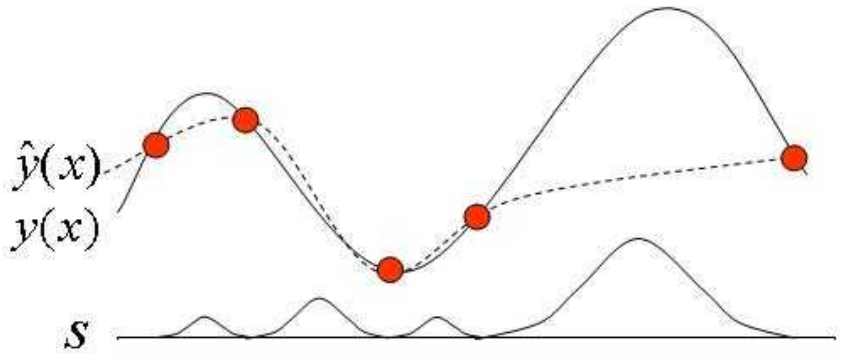

Figure 2-7 Concept of uncertainty

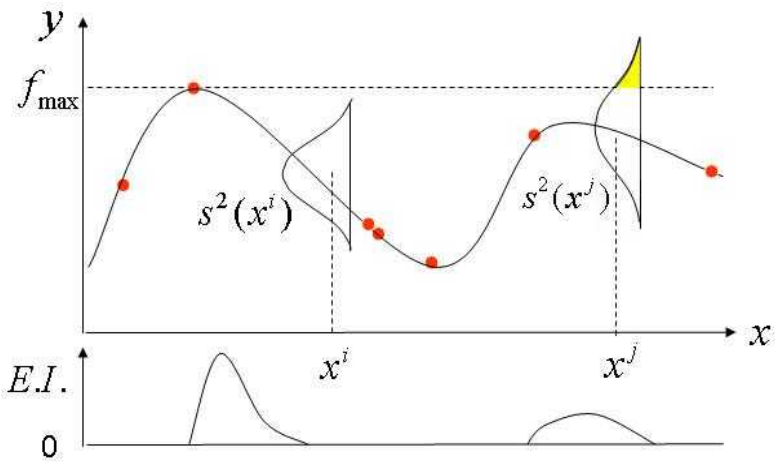

Figure 2-8 Concept of expected improvement

2.4 FEFLO

The flow solver used to predict pressure on windows and buildings is called FEFLO, a general-purpose CFD code based on the following principles:

1. Use of unstructured grids (automatic grid generation and mesh refinement)
2. Separate flow modules for compressible and incompressible flows
3. Finite element space discretization
4. ALE formulation for body fitted moving grids
5. Embedded formulation for complex/dirty geometries
6. Edge-based data structures for speed
7. Optimal data structure for different computer architecture
8. Bottom-up coding from the subroutine level to assure an open-ended, expandable architecture

The governing equations for the compressible, inviscid flow are the Euler equations, given by:

Continuity equation;
$$\frac{\partial \rho}{\partial t} + \frac{\partial (\rho u_i)}{\partial x_i} = 0 \tag{2-11}$$

Momentum equations;
$$\frac{\partial (\rho u_i)}{\partial t} + \frac{\partial (\rho u_i u_j)}{\partial x_j} = -\frac{\partial p}{\partial x_i} \tag{2-12}$$

Energy equation;
$$\frac{\partial (\rho e)}{\partial t} + \frac{\partial (u_j (\rho e + p))}{\partial x_j} = 0 \tag{2-13}$$

Here, pressure is calculated as follows under the assumption of an ideal gas.

$$p = (\gamma - 1)\rho \left[e - \frac{1}{2} u_j u_j \right] \tag{2-14}$$

FEFLO solves the above system using the Galerkin weighted residual method with explicit Taylor-Galerkin timestepping scheme. For a flux limiter, the Flux-Corrected Transport (FCT) scheme is employed [25], as it offers the best compromise of accuracy and speed for its class of problems. The flow solver advances the solution in time until all pressure waves exit a specified domain. The code has a long history of relevant blast simulation [2][3][4][5][6][7][8][9][24]. FEFLO is also equipped with automatic grid generation. The computational mesh is generated for every case in order to capture physics of shock wave precisely with fine mesh around blast location. One example of the special grids for this solver is shown in figure 2-9. Using this solver, it takes 9-12

hours on a 4 processor, shared memory machine (Intel Itanium II SGI Altix using the Intel Compiler) for a single run.

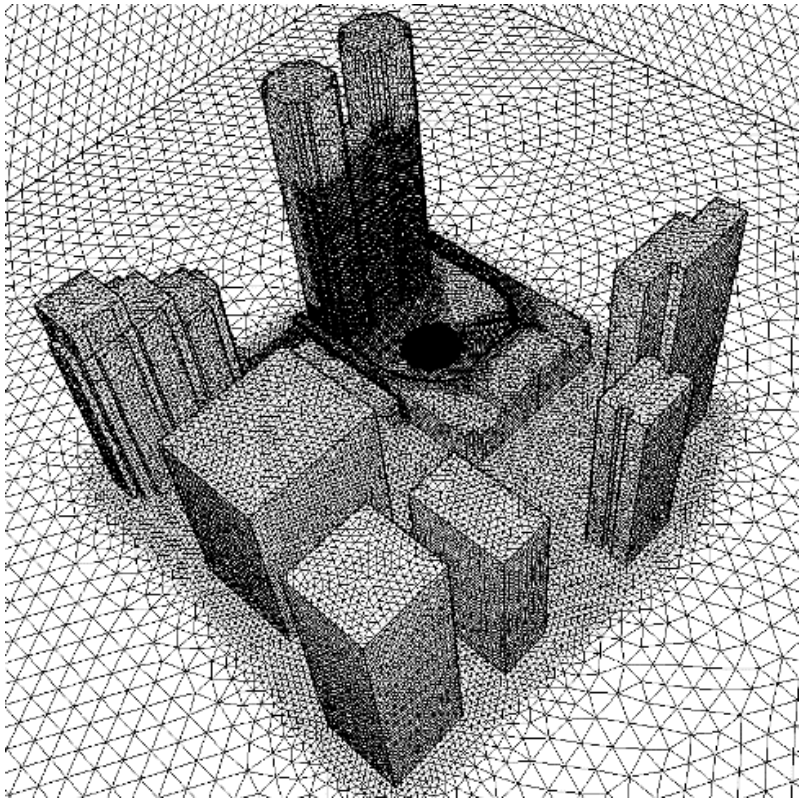

Figure 2-9 Example of spatial grid

3. Application to an analytical function

In this chapter, entire approach is applied with an analytic objective function that resembles the realistic problem in order to verify that it really works as a part of debug and development. The following checkpoints are carefully examined.

1. Whether the Kriging model reconstructs the response surface from highly constrained sample points.
2. Whether uncertainties and expected improvements give reasonable values at the right location.
3. Whether the maximum expected improvement converges to 0 after some samplings.
4. Whether a MOGA can find the Pareto front correctly.

3.1 Implementation

In order to answer these questions, a Multi-objective optimization of a multi peak test functions is conducted. The functions are expressed in equation 3-1 and 3-2. Figure 3-1 illustrates geometry and randomly selected initial 50 sample points of the test function.

$$\begin{aligned} func1 = \max\left(0, \frac{1}{3000}((x-3500)^2 + (y-3500)^2) + 2500\right) \\ + \max\left(0, \frac{1}{3000}((x-6500)^2 + (y-6500)^2) + 1500\right) \end{aligned} \tag{3-1}$$

$$
\begin{aligned}
func2 = \max\left(0, \frac{1}{3000}((x-3500)^2 + (y-3500)^2) + 1000\right) \\
+ \max\left(0, \frac{1}{3000}((x-3500)^2 + (y-6500)^2) + 2000\right) \\
+ \max\left(0, \frac{1}{3000}((x-7000)^2 + (y-6500)^2) + 1500\right)
\end{aligned}
\tag{3-2}
$$

Here maximums are at [3500,3500] and [3500,6500]. Its appearance is shown in figure 3-2.

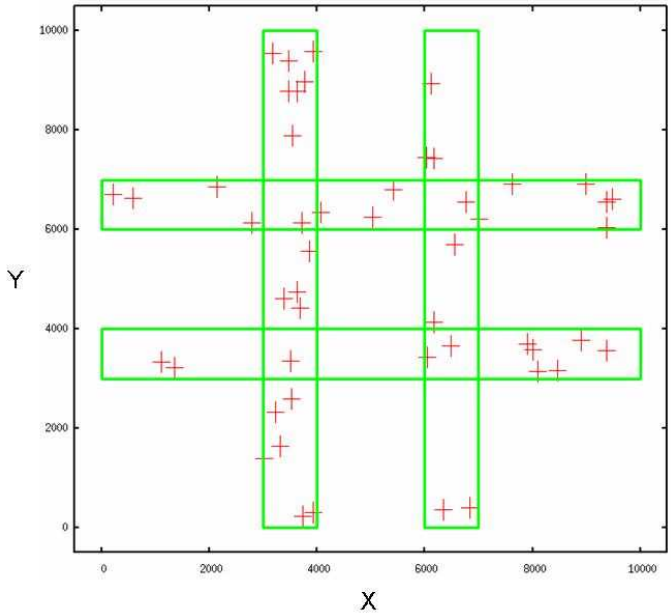

Figure 3-1 Geometry and Initial sample points

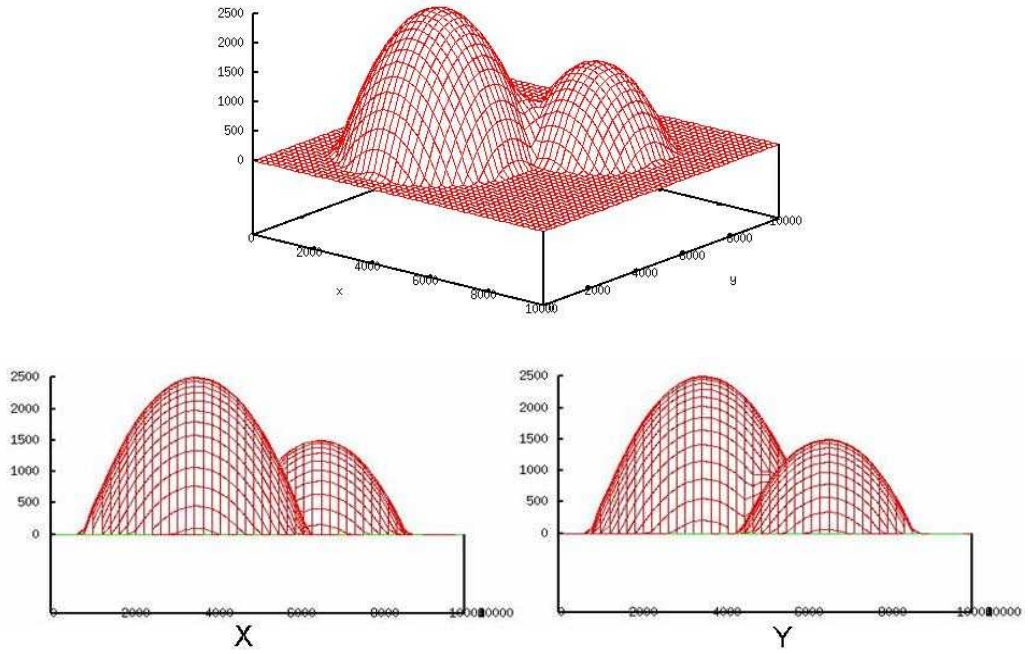

(a) Objective 1

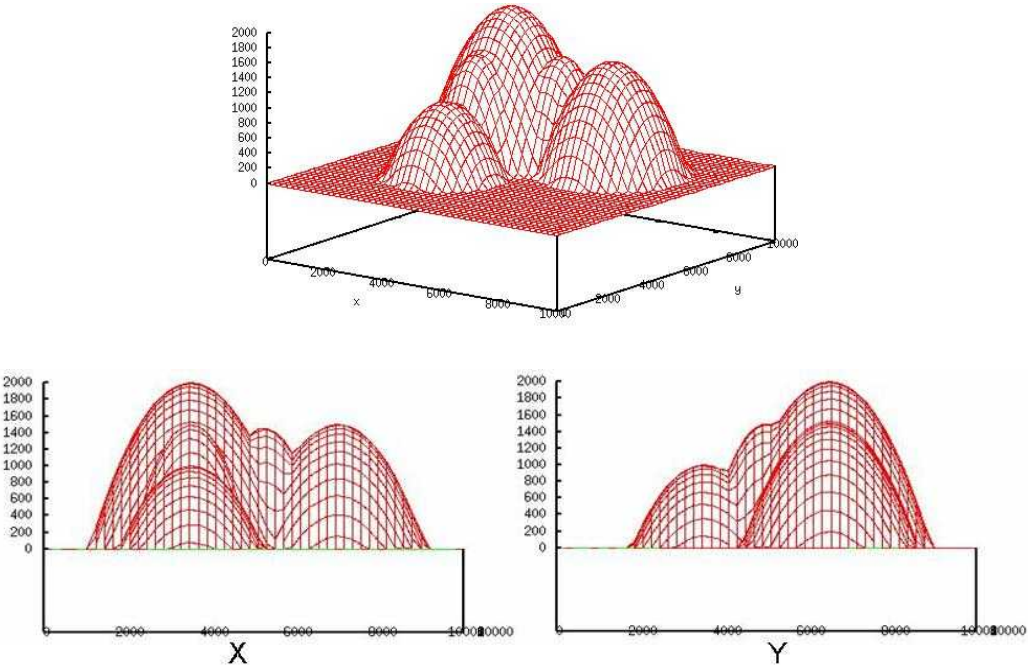

(b) Objective 2

Figure 3-2 Appearance of objective functions

3.2 Results

With a highly restricted geometry, the Kriging predictor successfully developed the approximation surfaces (figure 3-3). Figure 3-4 illustrates uncertainty and expected improvement of first objective in design space. Black represents low uncertainty (accurate). Compared to Figure 3-1, the black areas perfectly matches sampled locations and the red areas matches sparsely sampled areas, which means uncertainty is calculated correctly. Considering the uncertainty distribution and the fact that the prediction in figure 3-3(a) of the peak region around [3300, 3500] is incorrect, the expected improvement is maximized at a reasonable place. Figure 3-5 shows a transition of maximum expected improvement as the number of additional sample points increases. Each one successfully diminished to zero after the 59^{th} and 58^{th} sample. Figure 3-6 shows Pareto solutions obtained by MOGA with 6,000 evaluations and by 100,000 randomly picked evaluations. MOGA was able to find the entire Pareto front efficiently without bias in any particular region.

Since each location has multiple uncertainties corresponding to objective functions, normalizations are necessary to compare these values. This normalization is performed by simply removing the $\hat{\sigma}^2$ in (9). Once the Pareto solutions are obtained, a point with a maximum normalized uncertainty among them is selected for the next sampling. This process is continued until it is reduced more than 30% of the beginning.

In this test, after an additional sample, the maximum normalized uncertainty dropped from 0.12 to 0.015, which stopped the process.

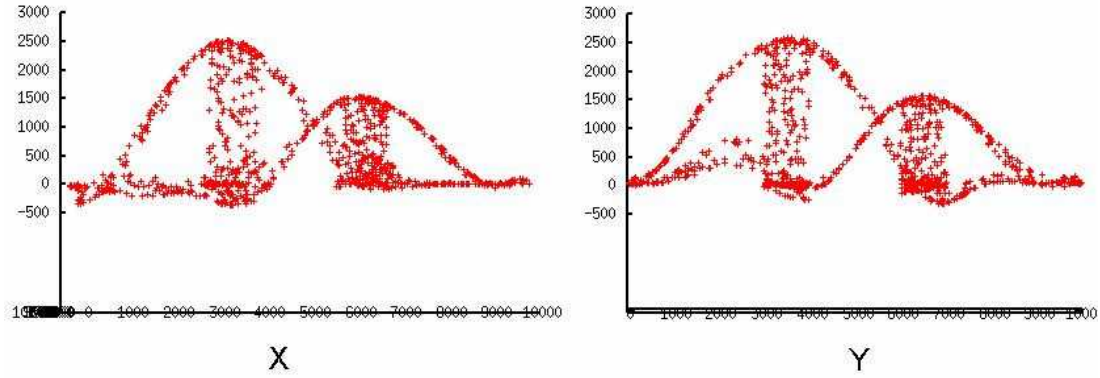

(a) Objective 1

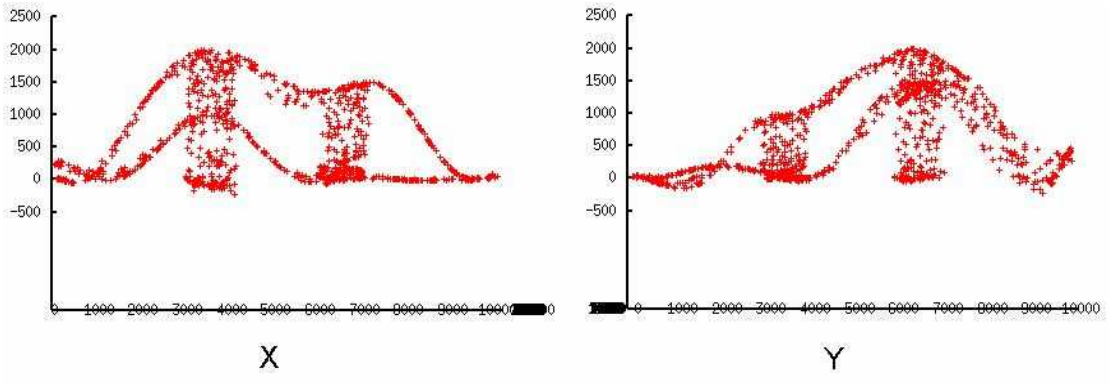

(b) Objective 2

Figure 3-3 Prediction of objective functions by Kriging model

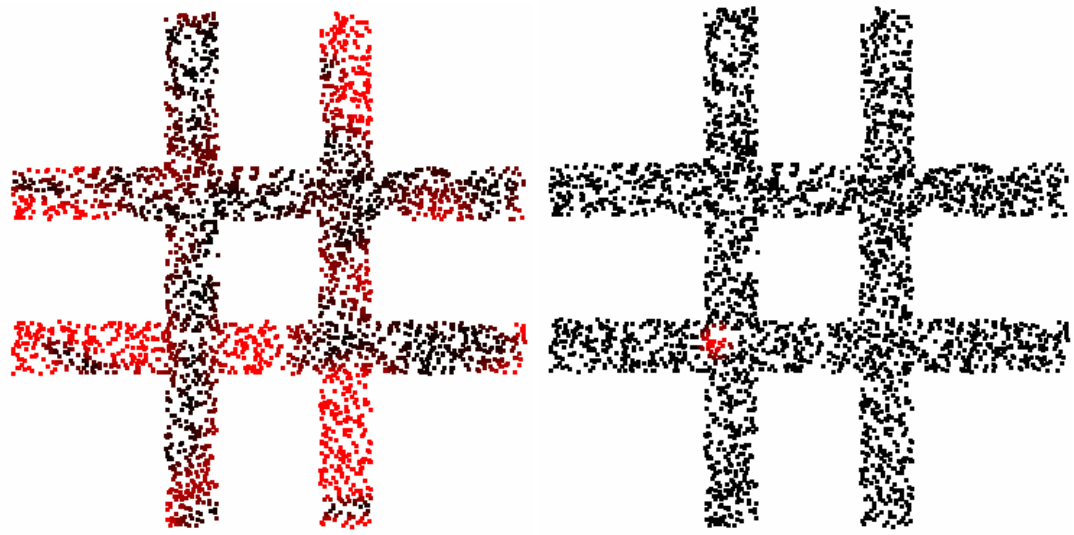

(a) Uncertainty (b) Expected Improvement

Figure 3-4 Distribution of Uncertainty and Expected Improvement

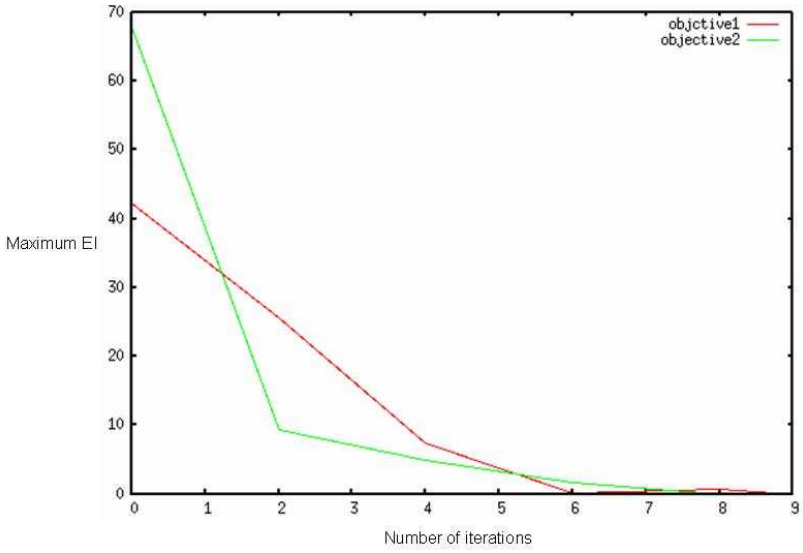

Figure 3-5 Transition of maximum Expected Improvement along number of additional samplings

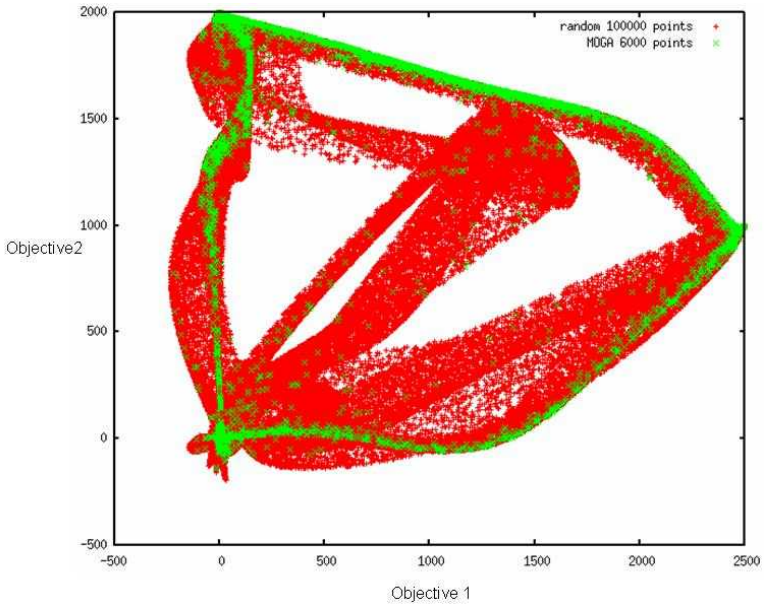

Figure 3-6 Pareto solutions obtained by random 1e5 and 6e3 MOGA points

4. Application to a blast simulation

4.1 Implementation

In this chapter, the entire framework is applied to a blast origin optimization problem. The target geometry is a place in front of Tokyo governor's office in Shinjuku-Japan, which is surrounded by many high-rise buildings. The geometry, shown in figure 4-1 was taken from Google-Earth. The image was read into the FEFLO pre-processor FECAD and the dimensions of the buildings corrected with Google-Earth. The geometry was then put into a computational box, and the boundary conditions, mesh size distribution in space and diagnostic information was specified. An initial mesh was generated for checking purposes. This process took one afternoon. 5,000 kg of TNT bomb is assumed to be used for this simulation. As mentioned above, two damages, to people and buildings, are considered. Given an arbitrary blast origin, these damages are estimated by the number of probes where either pressure or impulse exceeds certain thresholds. In figure 4-2, probes are shown as colored dots. As a constraint, blast origin is limited inside public roads (figure 4-5), assuming terrorists use auto for attacking. Firstly 49 initial sample points were selected randomly.

4.2 Results

Expected improvement of the second objective decreased to zero favorably. Since the global peak region of the first objective is rather flat, the expected improvement did not decrease even after 15 additional samplings (figure 4-5). However, the potential increase in this region is considered small, and hence its effect on the Pareto front insignificant. In this study, further accuracy of the global peak was not pursued to save time and computational resources. Figure 4-3 shows the Pareto front with the Pareto front predicted by Kriging at this point. There are large deviations from sampled points at middle region of the Pareto front. This deviation is interpreted as uncertainties of the prediction. At this point, it is impossible to know which front (Kriging or observation) to trust because Kriging has uncertainties and possibly observation is not a Pareto front. Among the predicted Pareto front, the point with highest normalized uncertainty was sampled iteratively. After two iterations, the maximum normalized uncertainty dropped from 0.924 to 0.612. Figure 4-4 shows Pareto front at this time. The fact that the predicted Pareto front moved closer to observations indicates reduction of uncertainties. Figure 4-5 shows Pareto rank in the order of sampling. This indicates that most of the sampled points introduced by Kriging (after 50^{th}) are ranked within 3^{rd}, which is significantly better than initial samples.

Figure 4-6 and 4-7 show damage to people and buildings, namely number of damaged probes as mentioned above, against design space respectively. Figure 4-8 shows Pareto rank of all observations. Damaged windows and buildings caused by a Pareto solution with design variable [-10860, -18609] are illustrated in figure 4-9. Figures 4-10 and 4-11

show surface pressures for the blast that originates at this location. Proximity of blast location to buildings is important (in order to damage them). On the other hand, the amount of TNT selected is such that casualties occur in a large range, thus leading to higher casualties at locations different from those that inflict high damage to buildings. As a result of this tradeoff, a region independent from global peaks is on Pareto front.

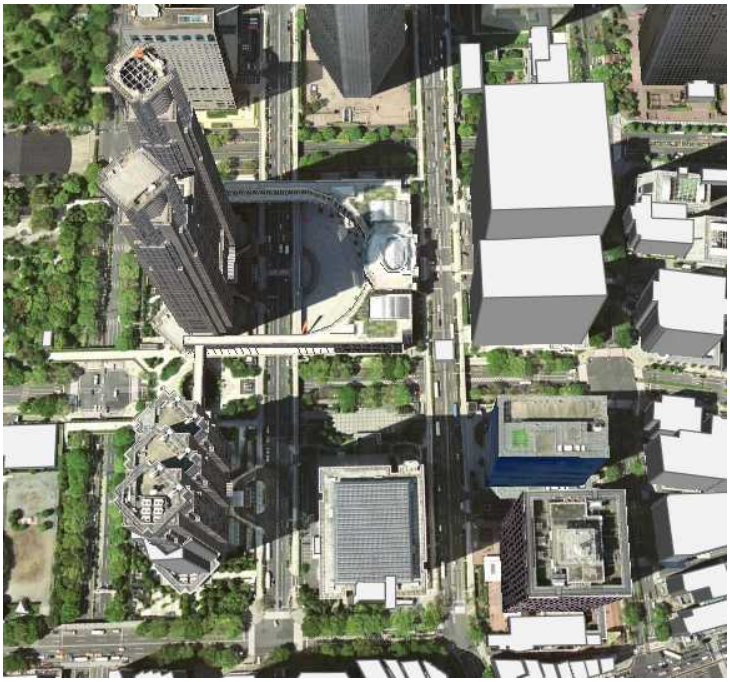

Figure 4-1 Overhead view from Google Earth

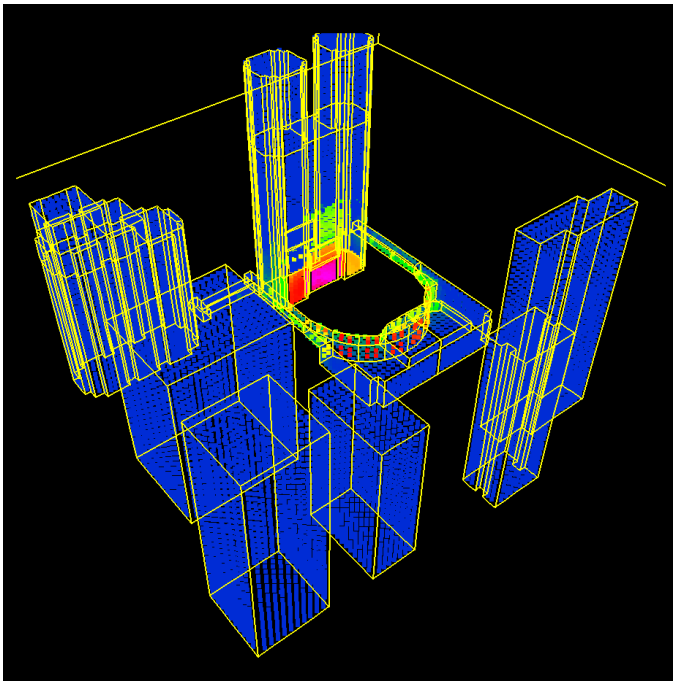

Figure 4-2 Probes

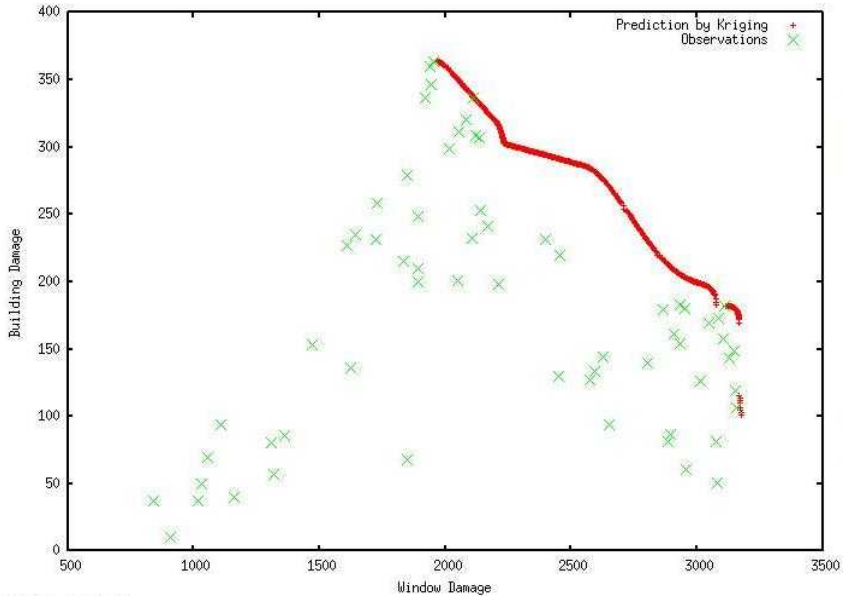

Figure 4-3 Pareto front with Kriging prediction after 1st step

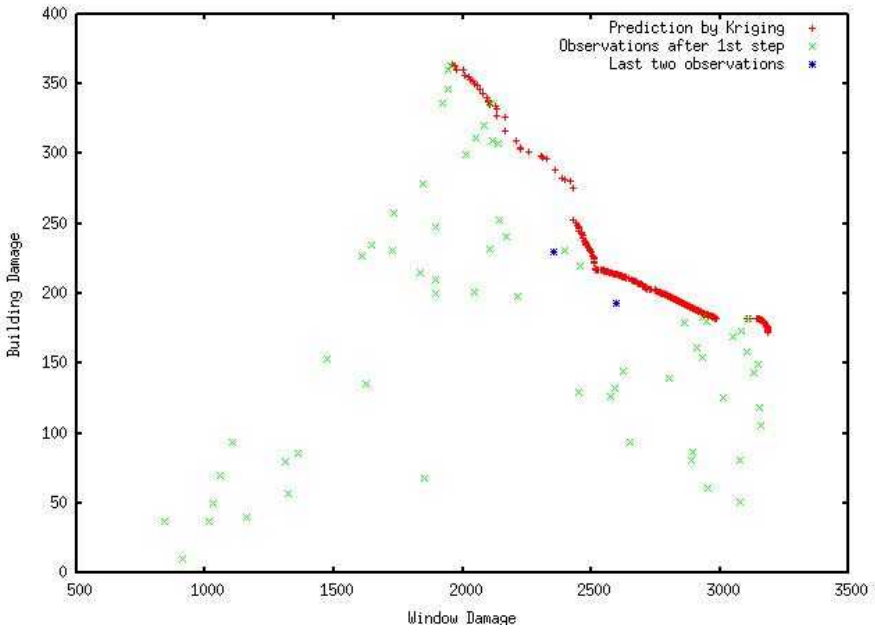

Figure 4-4 Pareto front with Kriging prediction after 2nd step

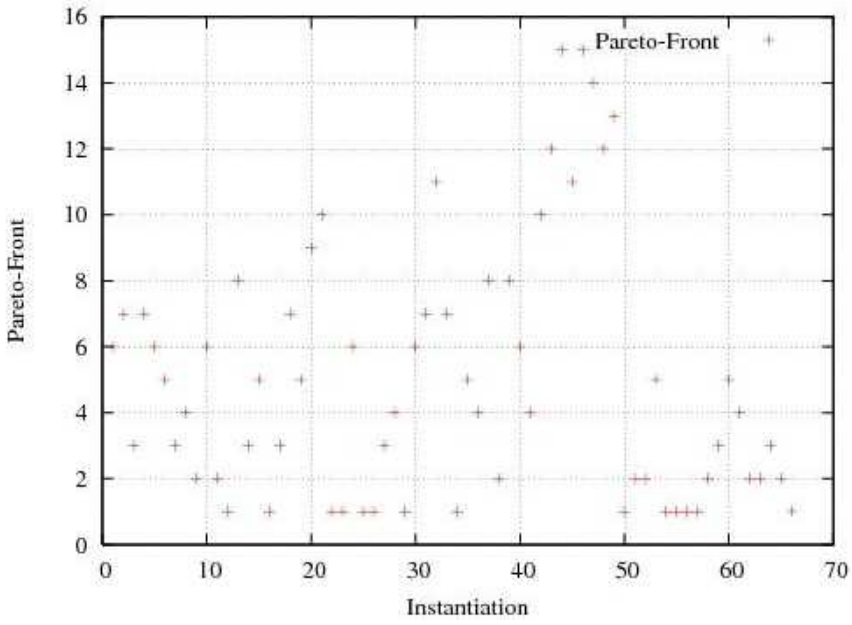

Figure 4-5 Pareto rank in the order of sampling

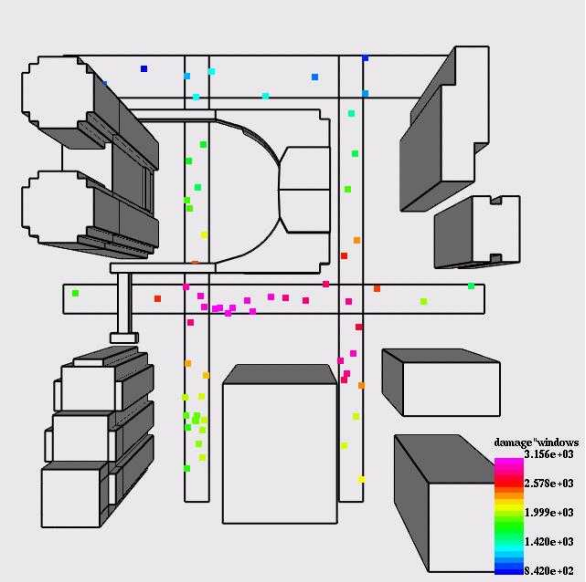

Figure 4-6 Damage to people

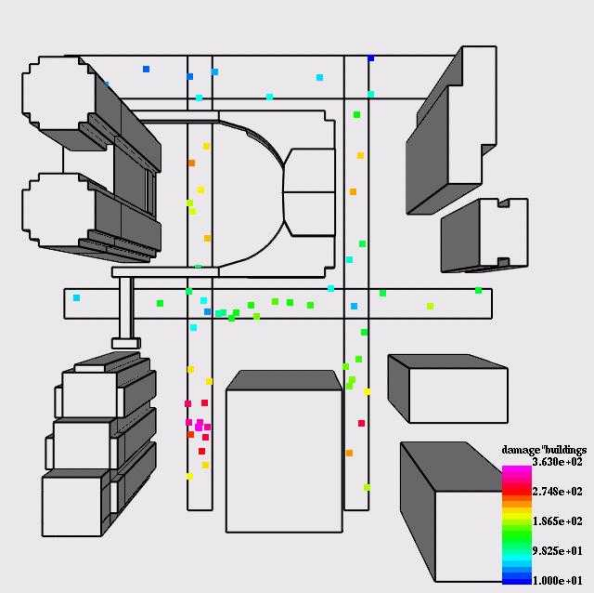

Figure 4-7 Damage to buildings

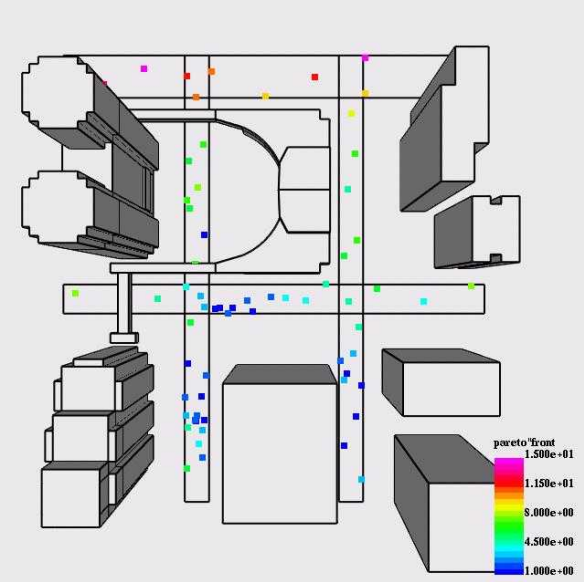

Figure 4-8 Pareto rank of sampled location

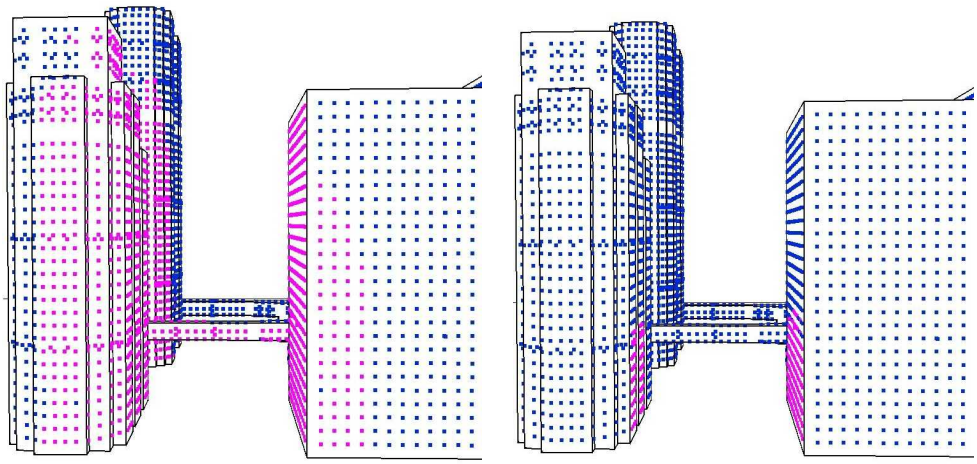

(a) Window (b) Building

Figure 4-9 Damages caused by a Pareto solution

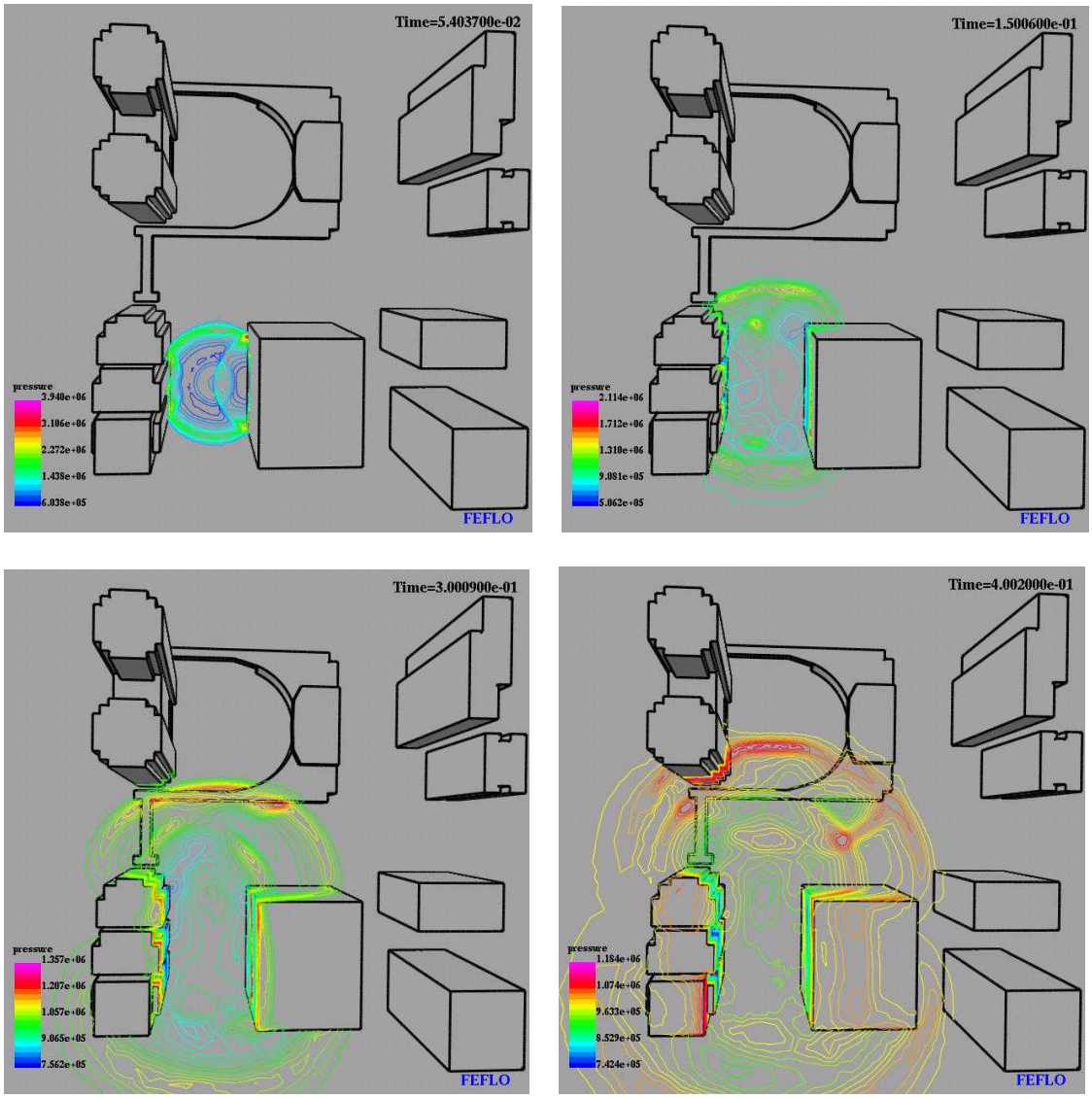

Figure 4-10 Surface pressure caused by a Pareto solution (top view)

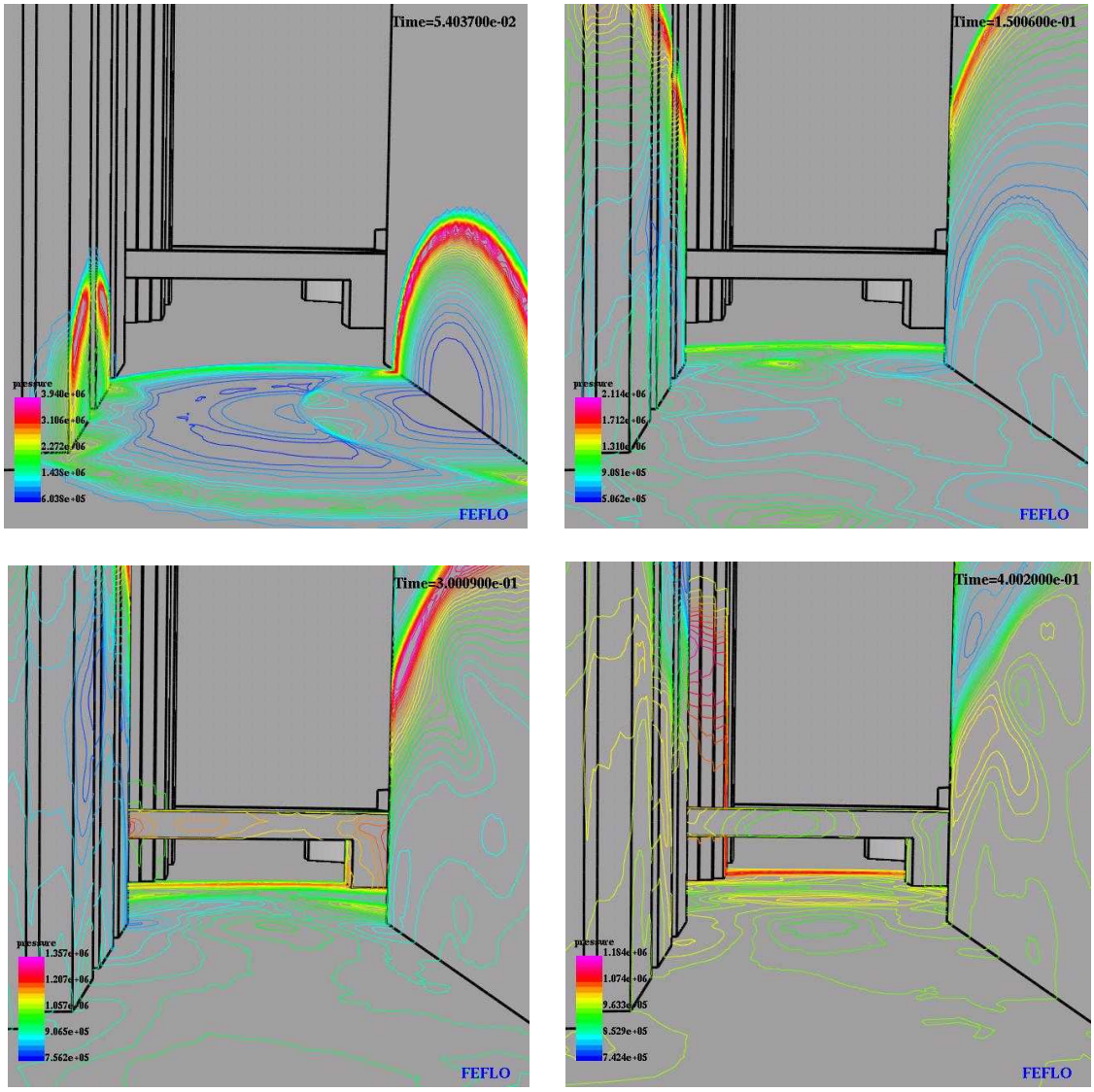

Figure 4-11 Surface pressure caused by a Pareto solution (side view)

5. Conclusions and future work

5.1 Conclusions

A multi objective optimization framework using a Kriging model has been developed for the approximation and optimization of complex spatial functions with multiple peaks. In a first step the potential global maxima of each objective are searched using the Kriging model. Thereafter the middle region of the Pareto front is explored.

The results indicate that only few sampling reduced prediction error at Pareto front greatly, yielding a more reliable Pareto front. The additional implementation after the 1st step requires MOGAs, which can be obtained from modified GAs.

5.2 Future work

Future work will focus on:

1. Damage criteria; especially coupling to Computational Structural Dynamics (CSD) is essential to estimate damage to buildings accurately.
2. Improved fidelity of flow physics; e.g. the entry of shocks into buildings.
3. Criteria for choosing sample points inside the Pareto front; there are multiple uncertainties corresponding to each objective function. Choosing one from them needs a criterion (in this study, the candidate which has maximum uncertainty).

BIBLIOGRAPHY

BIBLIOGRAPHY

[1] **A. Augugliaro, L. Dusonchet, E. Riva Sanseverino**, "Evolving non-dominated solutions in multiobjective service restoration for automated distribution networks" Electric Power Systems Research 59, pp.185–195(2001)

[2] **J.D. Baum and R. Löhner**, "Numerical Simulation of Shock Interaction with a Modern Main Battlefield Tank"; AIAA-91-1666(1991)

[3] **J.D. Baum, H. Luo and R. Löhner**, "Numerical Simulation of a Blast Inside a boeing 747" AIAA-93-3091(1993)

[4] **J.D. Baum, H. Luo and R. Löhner**, "Numerical Simulation of Blast in the World Trade Center" AIAA-95-0085(1995)

[5] **J.D. Baum, H. Luo, R. Löhner, C. Yang, D. Pelessone and C. Charman**, "A Coupled Fluid/Structure Modeling of Shock Interaction with a Truck" AIAA-96-0795(1996)

[6] **J.D. Baum, H. Luo, E. Mestreau, R. Löhner, D. Pelessone and C. Charman**, "A Coupled CFD/CSD Methodology for Modeling Weapon Detonation and Fragmentation" AIAA-99-0794(1999)

[7] **J.D. Baum, H. Luo, E.L. Mestreau, D. Sharov, R. Löhner, D. Pelessone and C. Charman**, "Recent Development of a Coupled CFD/CSD Methodology" AIAA-01-2618(2001)

[8] **J.D. Baum, H.Luo, E.L. Mestreau, D. Sharov, R. Löhner, D. Plessone and C. Charman**, "Recent Developments of a Coupled CFD/CSD Methodology for Simulating Structural Response to Airblast and Fragment Loading" Paper presented at ICCS 2001, San Francisco, CA, May(2001)

[9] **J.D. Baum, E.L. Mestreau, H.Luo, R. Löhner, D. Plessone and C. Charman**, "Modeling Structural Response to Blast Loading Using a Coupled CFD/CSD Methodology" Proc. Des. An. Prot. Struct. Impact/Impulsive/Shock Loads (DAOSIL), Tokyo, Japan, December(2003)

[10] **T.L. Bevins, B.J. Armstrong, J.T. Baylot, et al**. "Multiple building simulations and effect of beams behind blast barrier walls" In: Proceedings of the 2003 HPC user's group conference (DoD UGC_03), (2003)

[11] **D.D. Cox, and S. John**, "A statistical method for global optimization" in N. Alexandrov and M.Y. Hussaini, eds., *Multidisciplinary Design Optimization: State of the Art*, pp. 315–329, SIAM, Philadelphia. (1997)

[12] **N. Cressie**, "Geostatistics" *The American Statistician,* Vol. 43(4), pp. 197-202. (1989)

[13] **K. Deb**, "Multi-Objective Optimization Using Evolutionary Algorithms" J.Wiley & Sons (2001)

[14] **R. J. Donald, S Mathias and J. W. William**, "Efficient Global Optimization of Expensive Black-Box Function" Journal of Global Optimization, Vol. 13, pp. 455-492(1998)

[15] **C. M. Fonseca and P. J. Fleming,** "Genetic algorithms for multiobjective optimization: Formulation, discussion and generalization" in *Proc. 5th Int. Conf. Genetic Algorithms*, S. Forrest, Ed. San Mateo, CA: Morgan Kaufmann, pp. 416–423(1993)

[16] **S.E. Gano, J.E. Renaud, J.D. Martin and T.W. Simpson**, "Update Strategies for Kriging Models for Use in Variable Fidelity Optimization" 46th AIAA/ASME/ASCE/AHS/ASC Structures, Structural Dynamics, and Materials Conference; Austin, TX; USA; 18-21 Apr. 2005. pp. 1-20(2005)

[17] **A. Giotis, M. Emmerich, B. Naujoks, and K. Giannakoglou**, "Low cost stochastic optimization for engineering applications," in *Proc. Int. Conf. Evol. Methods Design, Opt. Control with Applicat. Ind. Prob*., pp. 361–366(2001)

[18] **D. E. Goldberg**, "Genetic Algorithms in Search, Optimization & Machine Learning. Reading" MA: Addison-Wesley (1989)

[19] **J.H. Holland**, "*Adaptation in Natural and Artificial Systems: An Introductory Analysis with Applications to Biology", Control, and Artificial Intelligence*. University of Michigan Press (1975)

[20] **S. Hosder, L.T. Watson, B. Grossman, W.H. Mason, H. Kim, R.T. Haftka and S.E. Cox**, "Polynomial response surface approximations for the multidisciplinary design optimization of a high speed civil transport" Technical Reports of NCSTRL at Virginia Tech CS(TR-01-03) (2001)

[21] **D. Huang, T. T. Allen, W. I. Notz, and N. Zheng, "**Global Optimization of Stochastic Black-Box Systems via Sequential Kriging Meta-Models" J Global Optim 34(3), pp. 441–466(2006)

[22] **S. Jeong, M. Murayama and K. Yamamoto**, "Efficient Optimization Design Method Using Kriging Model," Journal of Aircraft, Vol. 42 (2005), pp.413-420.

[23] **K. D. Jong, "**Evolutionary Computation: A Unified Approach" MIT Press (2006)

[24] **R. Löhner**, "Applied CFD Techniques" J. Wiley & Sons (2001)

[25] **R. Löhner**, K. Morgan, J. Peraire and M. Vahdati, "Finite Element Flux-Corrected Transport (FEM-FCT) for the Euler and Navier-Stokes Equations" ICASE Rep. 87-4, Int. J. Num. Meth. Fluids 7, 1093-1109 (1987)

[26] **J. I. Madsen, W. Shyy, and R. T. Haftka**, "Response surface techniques for diffuser shape optimization," *AIAA Journal* vol. 38, no. 9, pp. 1512–1518, (2000)

[27] **D. McGrath, C. Zhang, O.T. Carton**, "Geostatistical analyses and hazard assessment on soil lead in Silvermines area", Ireland. Environ. Poll. 127, 239–248.(2004)

[28] **R.H. Myers and D. C. Montgomery**, "Response Surface Methodology: Process and Product Optimization Using Designed Experiments" John Willy & Sons, New York (1995)

[29] **S. Obayashi, S. Takahashi, and Y. Takeguchi**, "Niching and elitist models for MOGAs," in *Parallel Problem Solving from Nature—PPSN V*. Berlin, Germany: Springer, 1998, pp. 260–269. (Lecture Notes in Computer Science).

[30] **A. Oyama, S. Obayashi and T. Nakamura**, "Real-coded adaptive range genetic algorithm applied to transonic wing optimization" Appl Soft Compting 16: 1–9 (2001)

[31] **T.A. Rose, P.D. Smith, S.A. Forth**, "Development of an adaptive mesh CFD code for high explosive blast simulation". In:12th International Symposium on Interaction of the Effects of Munitions with Structures, 2005

[32] **W.J. Roux, N. Stander, and R.T. Haftka**, "Response Surface Approximations for Structural Optimization," *6th AIAA/USAF/NASA/ISSMO Symp. on Multidisciplinary Analysis and Optimization*, Bellevue, WA, AIAA, Inc., Vol. 1, pp. 565-578.(1996)

[33] **J. Sacks, W.J. Welch, T.J. Mitchell and H.P. Wynn**, "Design and analysis of computer experiments (with discussion)" *Statistical Science* 4: 409–435(1989)

[34] **D. Sasaki, S. Obayashi and K. Nakahashi**, "Navier-Stokes Optimization of Supersonic Wings with Four Objectives Using Evolutionary Algorithm" Journal of Aircraft Vol.39, No.4 (2002) 621–629

[35] **D. Sasaki, S. Obayashi, K. Sawada and R. Himeno**, "Multiobjective Aerodynamic Optimization of Supersonic Wings Using Navier-Stokes Equations" Proc. of ECCOMAS 2000 [CD-ROM] (2000)

[36] **M. Schonlau**, "*Computer experiments and global optimization"* Ph.D. Thesis, University of Waterloo, Waterloo, Ontario, Canada. (1997)

[37] **N. Srinivas and K. Deb**, "Multiobjective optimization using nondominated sorting in genetic algorithms," *Evol. Comput.*, vol. 2, no. 3, pp. 221–248, (1994)

[38] **B.E. Stuckman**, "A global search method for optimizing nonlinear systems" *IEEE Transactions on Systems, Man, and Cybernetics* 18: 965–977. (1988)

[39] **F. Togashi, R.** Löhner**, J.D. Baum, H. Luo and S. Jeong,** "Comparison Of Search Algorithms For Assessing Airblast Effects" 17th AIAA Computational Flow Dynamics Conference; Toronto, Ontario; Canada; 6-9 June 2005. pp. 1-15. (2005)

[40] **Z. Z. Zhou, Y. S. Ong, P. B. Nair, A. J. Keane and K.Y. Lum**, "Combining global and local surrogate models to accelerate evolutionary optimization", *IEEE Trans. Systems, Man, and Cybernetics – Part C*, in press, (2005)

CURRICULUM VITAE

Toshihiro Tsuga graduated in 2001 from Sanda Gakuen High School, Hyogo, Japan. He received his Bachelor of Engineering from Tohoku University, Japan, in 2005. He received his Master of Science in Computational Science from George Mason University in 2007.